China Geology 6 (2023) 85–99

China Geology

Journal homepage: http://chinageology.cgs.cn
https://www.sciencedirect.com/journal/china-geology

Petrological and geochemical characteristics of mafic rocks from the Neoproterozoic Sugetbrak Formation in the northwestern Tarim Block, China

Hong-zhe Xie, Xiang-kun Zhu*, Xun Wang, Yuan He, Wei-bing Shen

MNR Key Laboratory of Isotope Geology, *MNR Key Laboratory of Deep-Earth Dynamics*, *Institute of Geology*, *Chinese Academy of Geological Sciences*, *Beijing* 100037, *China*

ARTICLE INFO

Article history:
Received 7 January 2021
Received in revised form 22 August 2021
Accepted 12 November 2021
Available online 25 November 2021

Keywords:
Mafic rocks
Sugetbrak Formation
Rodinia supercontinent
Neoproterozoic
Sr-Nd-Pb isotopes
Mantle plume
Geological survey engineering
Tarim Block
Xinjiang

ABSTRACT

The Neoproterozoic Sugetbrak Formation in the Aksu area, which is located at the northwest margin of Tarim Block, comprises mafic rocks and provides key records of the evolution of the Rodinia supercontinent. However, the genetic relationship among these mafic rocks exposed in different geographical sections are still unclear. In this study, the petrology, geochemistry, and Sr-Nd-Pb isotope geochemistry of the mafic rocks exposed in the Aksu-Wushi and Yuermeinark areas have been studied in some detail along three sections. The authors found that the mafic rocks in these three typical sections were mainly composed of pyroxene and plagioclase, containing a small amount of Fe-Ti oxides and with typical diabasic textures. All the mafic rocks in this region also showed similar geochemical compositions. They were characterised by high TiO_2 contents (1.47%–3.59%) and low MgO (3.52%–7.88%), K_2O (0.12%–1.21%). Large ionic lithophile elements (LILEs) (Rb, Sr, and Cs) were significantly depleted. Meanwhile, high field strength elements (HFSEs) were relatively enriched. In the samples, light rare earth elements (LREEs) were enriched, while heavy rare earth elements (HREEs) were depleted. Based on the Zr/Nb, Nb/Y, and Zr/TiO_2 ratios, the Aksu mafic rocks belong to a series of sub-alkaline and alkaline transitional rocks. The mafic rocks along the three typical sections showed similar initial values of $^{87}Sr/^{86}Sr$ (I_{Sr}) (0.7052–0.7097) and $\varepsilon_{Nd}(t)$ (–0.70 to –5.35), while the Pb isotopic compositions with $^{206}Pb/^{204}Pb$, $^{207}Pb/^{204}Pb$ and $^{208}Pb/^{204}Pb$ values of 16.908–17.982, 15.487–15.721, 37.276–38.603, respectively. Most of the samples plot into the area near EM-Ⅰ, indicating that the magma of the mafic rocks might have derived from a relatively enriched mantle with some crustal materials involved. The geochemical element characteristics of most samples showed typical OIB-type geochemical characteristics indicating that the source region had received metasomatism of recycled materials. Combining with the regional geological background and geochemical data, we inferred that the mafic rocks of the Sugetbrak Formation in the Aksu area were formed in an intraplate rift environment. Summarily, based on our study, the mafic rocks of the Sugetbrak Formation in the Aksu area were derived from a common enriched mantle source, and they were product of a magmatic event during the rift development period caused by the breakup of the Rodinia supercontinent.

©2023 China Geology Editorial Office.

1. Introduction

Mafic dyke swarms record critical information regarding the timing and processes of continental break-ups, because they can be precisely dated, yield information on crustal thickness and mantle sources (Li ZX et al., 1996, 1999, 2003, 2008; Li XH et al., 2003, 2006; Veevers JJ et al., 1997; Wingate JA et al., 1998; Karlstrom KE et al., 2000; Li ZX and Powell CM, 2001; Direen N and Crawford A, 2003). Some researchers have noticed that a large number of mafic dyke swarms associated with the Rodinia supercontinent breakup developed in the Aksu area, northwest margin of Tarim Block (Chen Y et al., 2004; Zhang CL et al., 2004, 2006, 2007, 2009, 2011; Zhang ZY et al., 2009; Zhu WB et al., 2008, 2011; Xu B et al., 2005). The mafic rocks are distributed on different sections, almost all over the different layers of the Sugetbrak Formation. However, the widespread Neoproterozoic mafic dykes have still not been well studied. The formation ages of these mafic rocks were not well constrained, and the origin of the mafic rocks exposed in

First author: *E-mail address*: hongzhexie@163.com (Hong-zhe Xie).

* Corresponding author: *E-mail address*: xiangkun@cags.ac.cn (Xiang-kun Zhu).

Literary editor: Xi-jie Chen
doi:10.31035/cg2021067
2096-5192/© 2023 China Geology Editorial Office.

Copyright © 2023 Editorial Office of China Geology. Publishing services by Elsevier B.V. on behalf of KeAi Communications Co. Ltd.
This is an open access article under the CC BY-NC-ND License (http://creativecommons.org/licenses/by-nc-nd/4.0/).

different regions or different sections in the same region and their genetic relationship are not clear, either.

In this study, the authors focus on the petrology, geochemistry, and Sr-Nd-Pb isotope geochemistry of the mafic rocks exposed in the Aksu-Wushi and Yuermeinark areas along the northwest margin of the Tarim Block and provided new constraints on the petrogenesis and their genetic relationship.

2. Geological setting and previous works

2.1. Neoproterozoic strata in the Aksu area of the northwest Tarim Block

The Tarim Block is bound by the Tianshan Orogens to the south and Tibet Plateau to the north, covering an area of more than 0.6×10^6 km^2 (Fig. 1b). The Tarim Block is a major tectonic constituent of the Central Asian collage (Fig. 1a), and

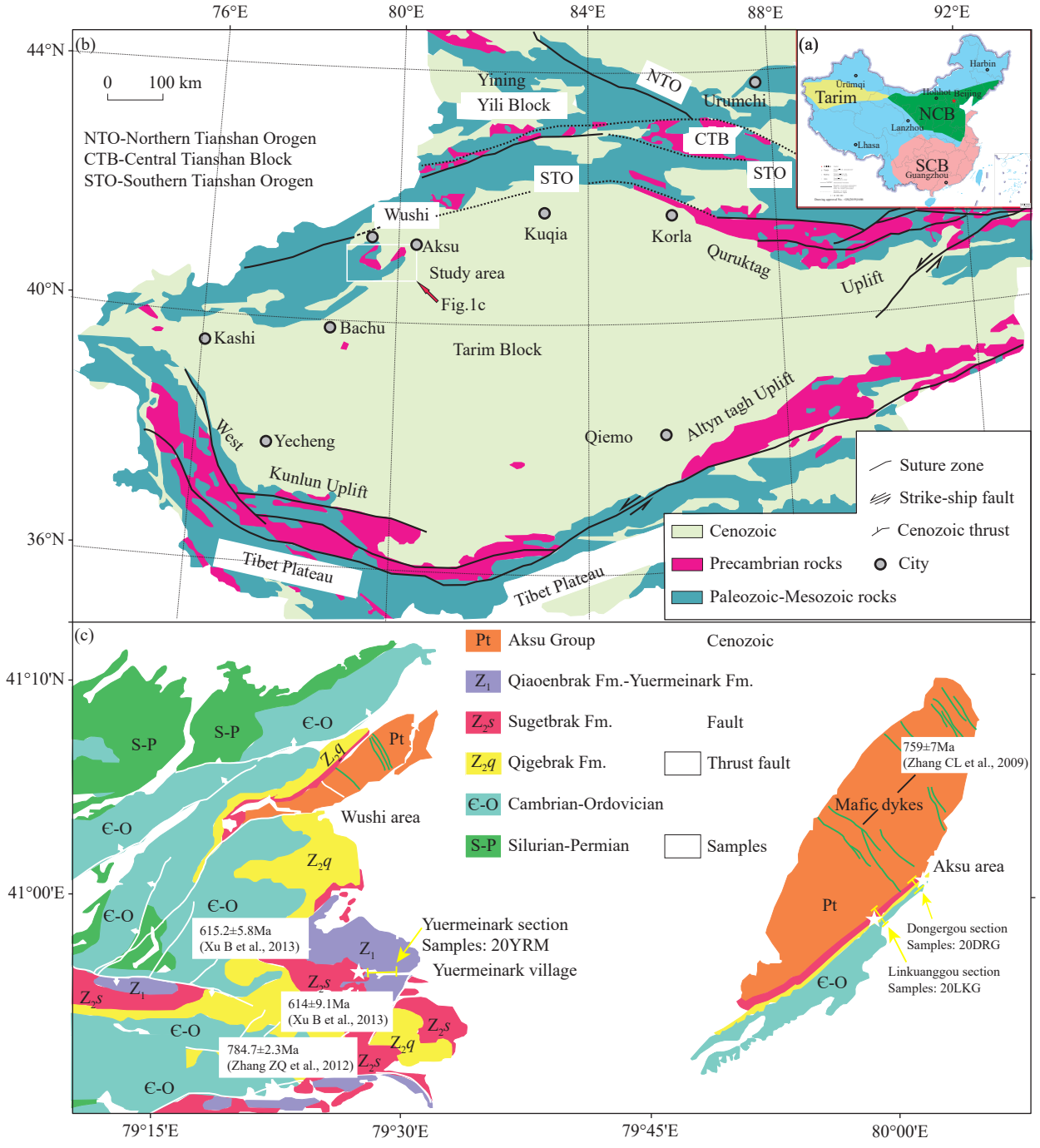

Fig. 1. Geological map of Tarim Block. a–Sketch map of China showing location of the Tarim Block in China. NCB: North China Block; SCB: South China Block (modified from Lu YZ et al., 2018, China basemap after China National Bureau of Surveying and Mapping Geographical Information); b–simplified geological map of the Tarim Block showing the distribution of Precambrian-Mesozoic rocks and the location of the Aksu-Wushi area (modified from Lu YZ et al., 2018); c–simplified geological map of the Aksu-Wushi area (modified from XBGMR, 1957; Lu YZ et al., 2018). Previous geochronological data of Precambrian mafic rocks and locations of samples and Fis 4a, b are indicated. Green line: mafic dykes.

it plays an important role in global tectonic framework. It is characterized by a double-layered structure, which consists of Precambrian basement and Neoproterozoic to Phanerozoic sedimentary cover sequences. The Precambrian basement rocks in the Tarim Block are mostly exposed along the northern (the Aksu and Quruqtagh areas), southwestern (the Tikelike area) and eastern (the Alytn Tagh Mountain and Dunhuang areas) margins (Fig. 1b; Lu YZ et al., 2008; Zhang CL et al., 2013; He JY et al., 2019).

In the Aksu area, which is located in the northwestern part of the Tarim Block (Fig. 1b), continuous outcrops of both the metamorphic basement and the Upper Neoproterozoic to Early Paleozoic successions are well exposed, and the strata were successively divided from bottom to top in the following order: the metamorphic rocks of the exposed basement of the Aksu Group, Neoproterozoic Qiaoenbrak Group, Yuermeinark Formation, Sugetebrak Formation, and Chigebrak Formation. The Aksu Group is mainly exposed in the Aksu-Wushi and Yuermeinark areas. It is composed of metasedimentary rocks and mafic schists, which undergo polyphase deformation in a subduction complex. The presence of blueschist facies attests to high-pressure and low-temperature metamorphism. The Aksu Group is considered as the oldest tectonic unit containing high-pressure metamorphic rocks. (Liou JG et al., 1989, 1996; Nakajima T et al., 1990; Zhu WB et al., 2011; Zhu GY et al., 2020). The metamorphic age of the Precambrian Aksu blueschist has been controversial, the youngest concordant detrital zircon ages in the Aksu Group indicate a maximum depositional ages of ca. 790–800 Ma (Lu YZ et al., 2017; Xia B et al., 2017) or ca. 730 Ma (Zhu WB et al., 2011). These orogenic events could have been related to the assembly of Rodinia. The Qiaoenbrak Group is exposed in the Yuermeinark area only, with a total thickness of 2000 m. It consists of a set of epimetamorphic sandstone and siltstone flysch at the lower and middle members formed in submarine gravity flow environment (Ding HF et al., 2015; Gao Z et al., 1986). The upper member of Qiaoenbrak Group is characterized by a set of diamictite and siltstone. The Yuermeinark Formation is a set of typical purplish-red diamictites considered to be continental glacial deposits and it can be generally correlated with the Tereen diamictite in the northeastern Tarim Block at top of the Cryogenian (Gao Z et al., 1986). The Sugetbrak Formation has intact strata exposed in the Aksu-Wushi and Yuermeinark areas, containing mafic rocks, red sandstones and gray mudstones, the overall thickness was approximately 400–450 m. The Sugetebrak Formation can be subdivided into two members: The lower member is composed of red conglomerates, red fluvial sandstones and gray lacustrine mudstones from bottom to top, interlaced with one to four layers of mafic rocks; the upper member is composed of gray calcirudite, quartz sandstone and red sandstone. The overlying strata of the Chigebrak Formation are a set of bedded micritic dolostone having a large number of Ediacaran stromatolites.

2.2. Petrography and geochronology of the mafic rocks

Different amounts of mafic rocks are exposed in the Sugetbrak Formation in the three sections in the Aksu-Wushi and Yuermeinark regions (Figs. 2a–d). Among them, the mafic rocks in the Dongergou section in the Wushi region is about 10 m thick, and four mafic dikes that intrude the sandstones of the Sugetbrak Formation are exposed in the Linkuanggou section; their thicknesses from the bottom to the top are 9 m, 20 m, 34 m, and 37 m, respectively. Three mafic dikes are exposed at the Yuermeinark section in the Yuermeinark area, with their thicknesses from the bottom to the top being 10 m, 12 m, and 50 m, respectively. They are interbedded with purplish-red sandstone, and there is no clear boundary between the various rock types, except for mafic rocks and sandstones. It is still controversial whether the mafic rocks in this area belong to extrusive origin or intrusive origin. However, based on our field investigation, the author find that the mafic rocks in the Sugetbrak Formation are most like mafic dikes intruding into surrounding rocks except the third set of mafic rocks at the top of the Yuermeinark section (Figs. 3a, b, d). In addition, there is baking phenomenon in the overlying strata and phase transformation in the edge and interior of some mafic rocks (Fig. 3c). No typical vesicular or amygdaloidal structures are observed in the Aksu-Wushi area.

The mafic rocks show different geological characteristics, and the author also observe that there are different layers of mafic rocks in different sections. However, the mineral assemblages of these rocks are very similar (Figs. 2e, f); the majority of the mafic rocks are mainly composed of plagioclase (45%–50%), pyroxene (45%–50%), and Fe-Ti oxides (magnetite and ilmenite) (5%), rare apatite, sphene and zircon that are present as accessory minerals. The mafic rocks generally show the diabasic texture and part of them show the poikilophitic texture (Figs. 2c, d). Most of the rocks have experienced low-temperature post-magmatic alteration, such as sericitization and clay formation.

The precise formation age of the Sugetbrak mafic rocks is still not well constrained. Wang F et al. (2010) conducted the first LA-ICPMS U-Pb dating on zircons from the mafic rocks of the Sugetbrak Formation. They obtained 17 zircons for U-Pb dating, which yielded ages ranging from 1945 Ma to 755 Ma, and these ages have been interpreted as the ages of Mesoproterozoic metamorphic zircons and Late Neoproterozoic inherited magmatic zircons, Zhang ZC et al. (2012) obtained a 783 ± 2.3 Ma zircon age for the lower layers of the mafic rocks of the Sugetbrak Formation by the LA-ICP-MS method and interpreted it as the crystallization age of the Sugetbrak mafic rocks. Xu B et al. (2013) reported SHRIMP zircon U-Pb ages of 615.2 ± 4.8 Ma and 614.4 ± 9.1 Ma, and they considered these ages as eruption age of the Sugetbrak Formation. Lu YZ et al. (2018) preformed the first $^{40}Ar/^{39}Ar$ dating on separated mineral grains from the Sugetbrak mafic rocks in the Aksu area, pyroxenes form a layered mafic rock within the Sugetbrak Formation yielded a $^{40}Ar/^{39}Ar$ plateau age of 521.0 ± 2.1 Ma. They considered that the mini-plateau age of 521.0 ± 2.1 Ma was a minimum crystallization age for mafic rocks of the Sugetbrak Formation.

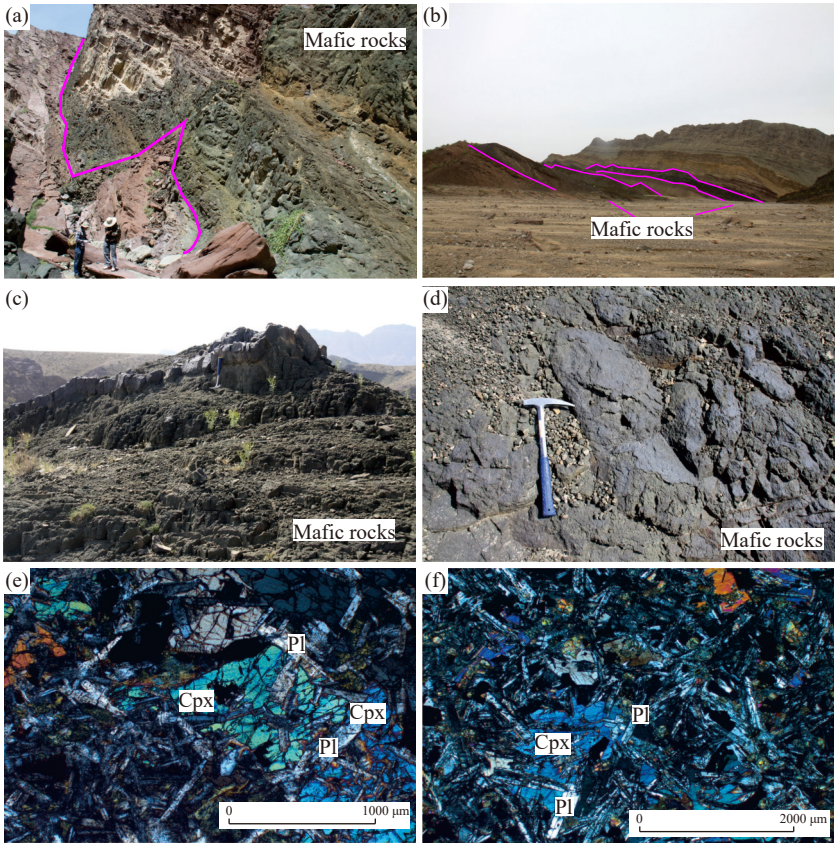

Fig. 2. Field occurrence and petrography of the mafic dykes in the Aksu. a–Field occurrence of the mafic rocks with massive structure in the Dongergou section; b–the mafic rocks in the Linkuanggou section showing the mafic rocks is consistent with the strata; c–the mafic rocks intruding into strata in the Yuermeinark section; d–field occurrence of the mafic rocks in the Yuermeinark section; e, f–photomicrographic image of the mafic rocks (cross-polarized light), Abbrevation; Cpx–clinopyroxene; and Pl–plagioclase.

3. Analytical methods

3.1. Sample preparation

Samples were taken from each set of mafic rocks in the Aksu-Wushi and Yuermeinak areas in three sections. After observation under a microscope, 18 relatively fresh samples were selected and sent to the Beijing Shougang Geological Survey Institute. The central part of the sample was used for whole-rock analysis. The sample was ground in a steel mortar using a 200 mesh in an agate grinding machine for analyzing the main and trace elements. A total of eight samples were selected from the three sections for the Sr-Nd-Pb isotopic analysis.

3.2. Major and trace element analyses

The major and trace elements of the mafic rocks were analyzed at the Wuhan Sample Solution Analytical Technology Co., Ltd., in Wuhan, China. Major element analyses of the whole rock were conducted using X-ray fluorescence (XRF; Primus II, Rigaku, Japan), and the accuracy analysis (better than 1%), FeO was performed using the chemical volumetric method. $_{T}Fe_2O_3$ indicated the total amount of iron determined using the XRF spectrometer test, and the FeO content was obtained using a wet chemical analysis method. The trace element analysis of the whole rock was conducted using inductively coupled plasma mass spectrometry (ICP-MS) (Agilent 7700e), and the analysis accuracy was more than 3%. The analysis process was monitored according to international standards.

3.3. Sr-Nd-Pb isotope analyses

The pre-treatment and testing of the Sr-Nd-Pb isotope were completed at the Wuhan Shanghai Spectroscopic Analysis Technology Co., Ltd., Hubei, China by using the Neptune Plus Multicollector ICP-MS (MC-ICP-MS) instrument (Thermo Fisher Scientific, Dreieich, Germany). The Sr and Nd isotope ratios were standardised to be $^{87}Sr/^{88}Sr=0.1194$ and $^{146}Nd/^{144}Nd=0.7219$, respectively. Li CF et al. (2012) conducted a detailed test; one international National Institute of Standards and Technology (NIST; SRM 987) standard was measured for every ten samples analysed. Analyses of the NIST SRM 987 standard solution yielded $^{87}Sr/^{86}Sr$ ratios of 0.710244 ± 22 (2SD, n=32), which were identical to the values in previous studies (0.710241 ± 12; Thirlwall, 1991). One JNdi-1 standard was measured for every ten samples analysed. Analyses of the JNdi-1 standard yielded the $^{143}Nd/^{144}Nd$ ratio of 0.512118 ± 15 (2SD, n=31), which shows an error comparable to those found in other published studies (0.512115 ± 07; Tanaka T et al., 2000). This indicates the stability of the instrument and the reliability of the calibration strategy. Pb isotope analysis uses Hf to

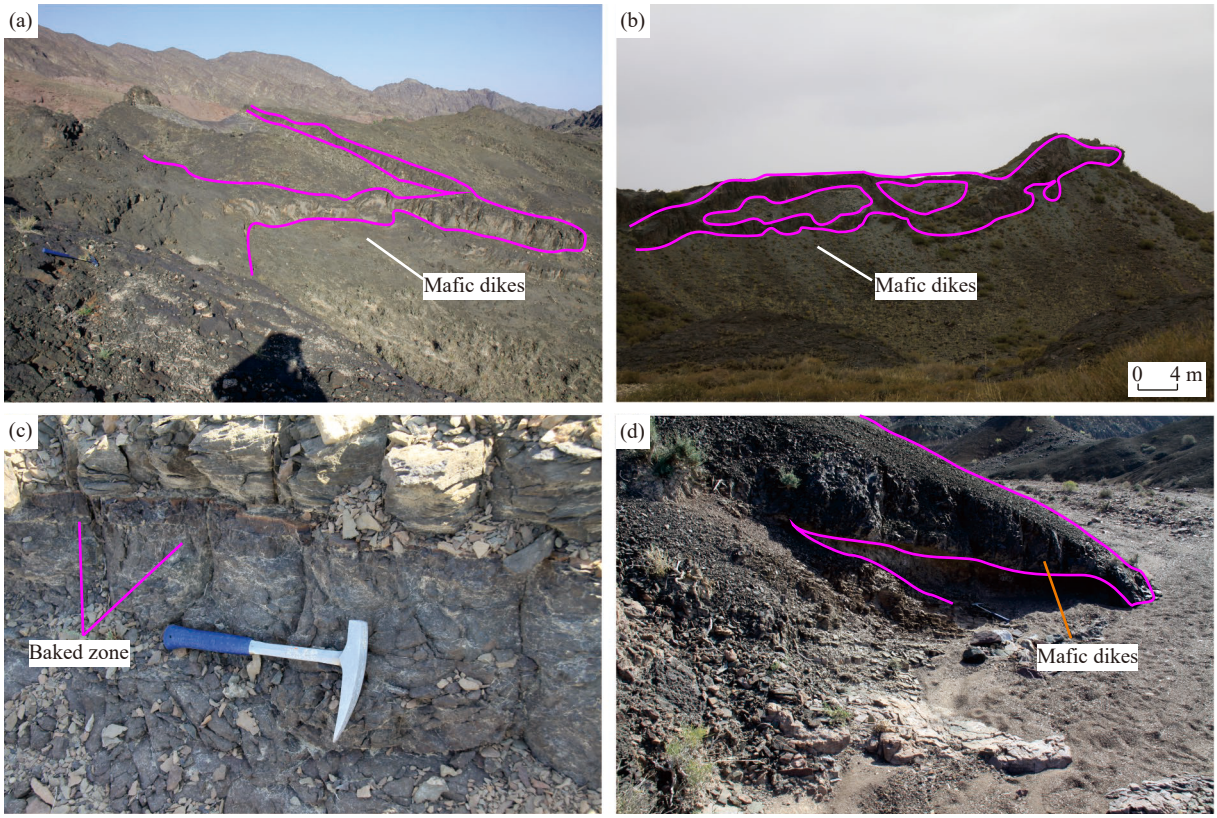

Fig. 3. Field occurrence the mafic dikes in the Aksu. a–Mafic dikes in the Dongergou section; b–the mafic dikes intruding into strata in the Yuermeinark section; c–the baking phenomenon of mafic dikes to the upper strata in the Linkuanggou section; d–the mafic dikes intruding into strata in the Linkuanggou section.

completely dissolve the powder sample under high temperature and pressure, and the Pb samples are separated and purified using a centrifugal column. The data were derived from a large number of tests according to a Pb standard (NBS SRM 918); one NBS SRM 981 standard was measured for every ten samples analysed. Analyses of the NBS SRM 981 standard yielded an external precision of 0.03% (2RSD) for the $^{20x}Pb/^{204}Pb$ ratios. All the measured $^{20x}Pb/^{204}Pb$ ratios of unknown samples were normalised to the well-accepted NBS SRM 981 standards of $^{208}Pb/^{204}Pb$ = 36.7262 ± 31, $^{207}Pb/^{204}Pb$ = 15.5000 ± 13 and $^{206}Pb/^{204}Pb$ = 16.9416 ± 13 (Baker J et al., 2004).

4. Results

4.1. Major and trace element geochemistry

The major element compositions of the representative samples from the mafic rocks are listed in Table 1. Most samples showed high loss on ignition (LOI) values (2.81%–7.49%), especially the sample 20LKG-1 (LOI values of 11.42%), which indicated that they experienced significant post-magmatic alteration. The samples displayed varying contents of SiO_2 (38.35%–59.8%); contents of TiO_2 (1.47%–3.59%), $_TFe_2O_3$ (7.43%–16.41%), and Al_2O_3 (14.32%–16.94%); and low contents of MgO (3.52%–7.88%), K_2O (0.12%–1.21%), and P_2O_5 (0.32%–0.67%). The Na_2O content was higher than the K_2O content. The $Mg^{\#}$ value (=100×MgO/(MgO+FeO)) ranged from 34% to 51%. In Harker diagrams (Fig. 4), Al_2O_3, K_2O, MgO and Na_2O contents of the Sugetbrak mafic rocks display positive correlations with SiO_2 contents, whereas TiO_2, Fe_2O_3, CaO and MnO contents exhibit negative correlations. It can be seen from the Harker diagram, the chemical composition of mafic rocks in the Sugetbrak Formation in the Aksu area was basically similar and has certain correlation (Fig. 4).

Rare earth elements (REEs) and other trace elements contents of mafic rocks are listed in Table 2. All the samples showed similar trends. Since most of the samples have been altered to different degrees in the later period, some of the samples showed highly negative anomalies of K and Sr. The content of REEs in all the samples was relatively high, as shown in the chondrite-normalized REE patterns (Fig. 5a), which indicated all the samples were enriched in light rare earth elements (LREEs) relative to heavy rare earth elements (HREEs). Additionally, some samples showed a slightly negative Eu anomaly (δEu=0.82).

In the primitive mantle-normalized spidergram (Fig. 5b), samples from different areas of the Aksu exhibit similar characteristics. The samples showed depletion in large-ion lithophile elements (LILEs) and enrichment in high field elements (HFSEs), which was identical to the features of ocean island basalt (OIB)-type mafic rocks. In view of the alteration effects proved by high LOI values, to further determine the properties of the magmatic rocks, immobile trace elements (Nb and Y) were used to assess their alkali character. However, the use of the alkali *vs*. SiO_2 diagram (Le

Table 1. Major element abundances (%) of the Sugetbrak mafic rocks in the Aksu area, NW Tarim Block.

Sample	SiO_2	TiO_2	Al_2O_3	$_TFe_2O_3$	MnO	MgO	CaO	Na_2O	K_2O	P_2O_5	FeO	LOI	Total	Mg#	CaO/Al_2O_3
20LKG-1-1	38.35	2.50	14.19	10.13	1.18	4.09	12.33	4.16	0.65	0.34	2.70	11.42	99.35	42	0.87
20LKG-1-2	49.00	2.77	15.16	12.52	0.47	6.37	3.65	3.52	0.60	0.34	3.85	5.16	99.56	47	0.24
20LKG-2-1	42.09	3.11	15.73	14.13	1.89	5.76	4.50	4.48	1.11	0.48	4.90	6.39	99.66	41	0.29
20LKG-2-2	45.55	3.07	16.14	14.53	0.27	5.53	4.68	4.03	1.10	0.52	4.00	4.70	100.11	40	0.29
20LKG-3	44.84	3.01	15.88	15.30	0.30	5.26	6.23	4.21	0.92	0.50	6.00	3.43	99.87	36	0.39
20LKG-4-1	44.09	3.17	15.30	14.59	0.22	5.57	6.46	4.45	0.84	0.52	5.90	4.58	99.79	38	0.42
20LKG-4-2	44.78	2.86	15.35	15.40	0.17	5.69	6.08	4.21	0.87	0.45	6.00	3.89	99.74	38	0.40
20DRG-1-1	48.59	2.73	14.32	13.52	0.28	5.08	6.38	4.53	1.21	0.32	5.90	2.33	99.27	37	0.45
20DRG-1-2	47.04	3.00	16.25	13.81	0.21	7.88	0.95	5.20	0.72	0.40	3.55	4.32	99.78	51	0.06
20YRM-3-1	44.89	3.40	15.02	16.41	0.22	5.89	6.52	3.23	1.01	0.46	6.15	2.95	99.98	37	0.43
20YRM-3-2	48.54	2.95	16.94	12.28	0.19	5.06	7.93	3.03	0.86	0.41	3.65	2.04	100.22	42	0.47
20YRM-2-1	43.61	2.95	14.97	13.75	0.24	4.65	6.18	4.65	0.19	0.63	6.40	7.49	99.30	34	0.41
20YRM-2-2	46.35	2.96	14.25	13.70	0.19	5.80	4.88	4.38	0.34	0.57	6.25	6.60	100.01	40	0.34
20YRM-1-1	59.85	1.47	15.13	7.43	0.10	3.52	1.11	6.62	0.12	0.37	3.05	2.81	98.53	43	0.07
20YRM-1-2	44.70	3.59	14.76	14.48	0.61	5.45	5.24	4.68	0.23	0.67	6.00	5.26	99.66	38	0.35
20YRM-1-3	45.33	3.16	16.75	12.34	0.26	5.85	3.33	5.61	0.21	0.53	6.25	5.97	99.33	41	0.20
20YRM-1-4	50.06	2.29	16.19	10.73	0.26	4.08	2.91	4.90	0.64	0.43	5.45	5.35	97.83	36	0.18

Note: $Mg^{\#}$ = molecular proportion of MgO/(MgO + FeO), assuming 85% of total iron oxides as FeO. $Mg^{\#} = 100 \times [MgO]/\{[MgO]+[TFe_2O_3] \times 0.8998 \times 0.85\}$. if TFe_2O_3 is reported.

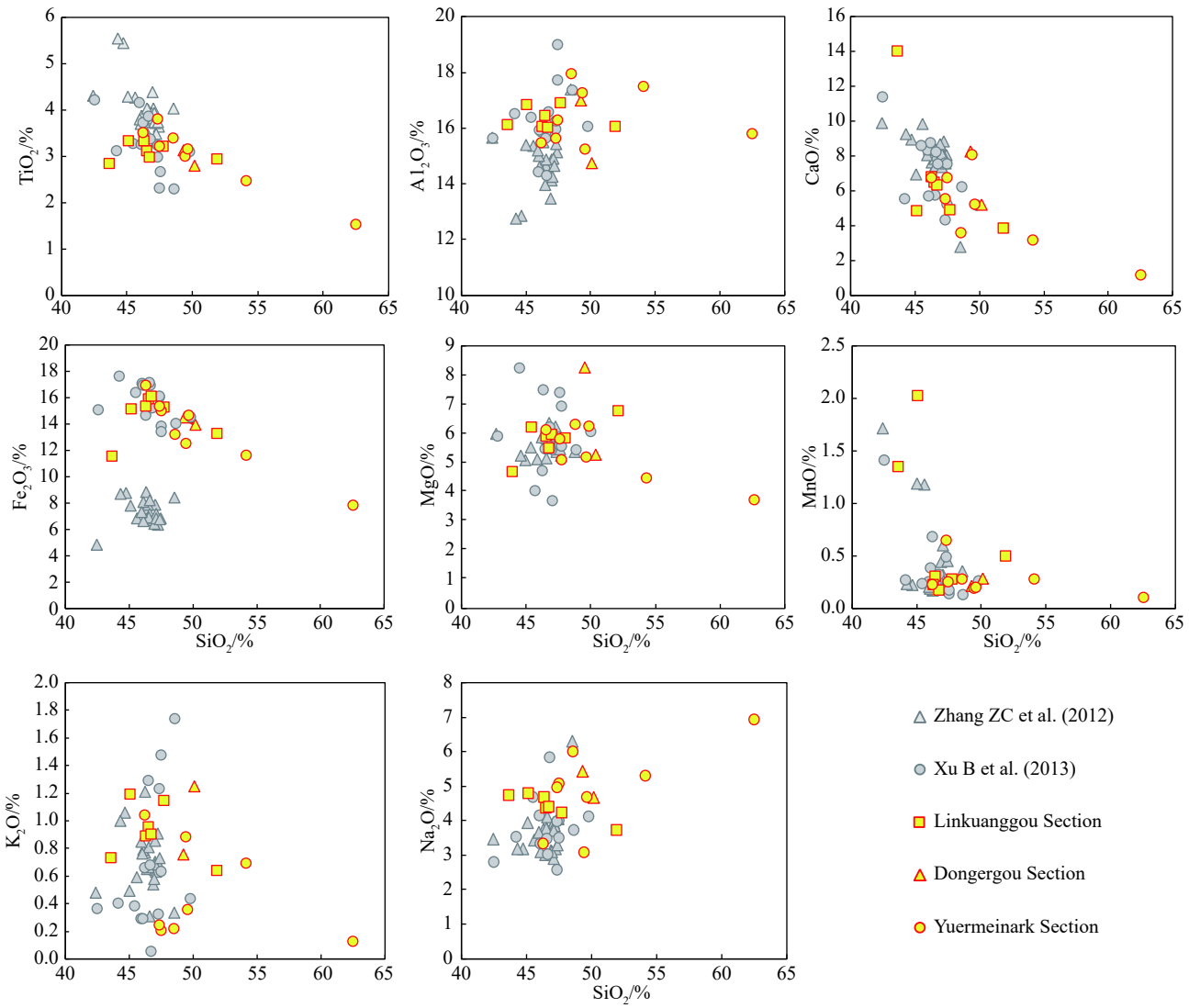

Fig. 4. Variation diagrams for major oxides *vs*. SiO_2 contents of the mafic rocks in the Aksu.

Table 2. Trace element abundances (10^{-6}) of the Sugetbrak mafic rocks in the Aksu area, NW Tarim Block.

Sample	20LKG-1-1	20LKG-1-2	20LKG-2-1	20LKG-2-2	20LKG-3	20LKG-4-1	20LKG-4-2	20DRG-1-1	20DRG-1-2	20YRM-4-1	20YRM-4-2	20YRM-2-1
Cs	0.34	0.70	0.39	0.28	0.97	1.64	2.09	0.20	0.21	0.26	0.12	0.31
Rb	7.60	9.69	21.52	12.98	13.35	12.23	13.77	15.96	5.67	12.71	14.88	3.69
Ba	170	158	412	454	550	511	517	905	1482	459	439	763
Th	2.17	2.03	2.33	2.54	2.67	2.05	2.30	2.19	2.37	2.18	2.05	2.52
U	0.55	0.62	0.73	0.73	0.67	0.52	0.60	0.68	2.14	0.55	0.47	0.75
Nb	19.04	18.45	25.01	27.77	27.17	25.33	25.20	20.10	21.24	25.16	22.14	26.81
Ta	1.11	1.06	1.49	1.67	1.66	1.52	1.50	1.19	1.26	1.53	1.32	1.63
K	5354	4997	9206	9089	7620	6998	7197	10061	5976	8400	7164	1560
La	24.90	23.10	26.32	28.60	28.25	28.66	26.70	25.08	19.15	27.36	23.44	32.77
Ce	51.90	48.86	56.19	62.31	61.13	60.98	57.01	51.43	42.95	57.12	50.03	70.69
Pb	379	2768	193	12.07	6.38	6.03	4.82	4.71	19.18	6.41	5.89	7.81
Pr	6.48	6.35	7.25	8.09	8.00	7.90	7.32	6.52	5.74	7.56	6.61	9.31
Sr	281	289	331	476	542	486	572	711	88.38	377	472	162
P	1483	1470	2112	2260	2195	2247	1950	1401	1758	1985	1798	2749
Nd	28.39	27.13	31.56	34.75	33.95	34.39	31.46	27.72	25.29	32.21	28.38	39.65
Zr	193	189	221	240	248	208	225	199	221	226	201	268
Sm	6.58	6.60	6.98	7.76	7.63	7.61	7.09	6.51	6.45	7.41	6.73	8.64
Eu	2.20	2.25	2.21	2.40	2.40	2.48	2.38	2.14	1.76	2.37	2.19	2.59
Ti	14987	16624	18632	18386	18050	18998	17133	16336	17961	20383	17679	17709
Dy	5.86	5.98	5.35	5.97	5.74	5.68	5.40	5.81	6.24	6.36	5.65	7.66
Y	31.77	32.27	27.72	30.79	30.03	29.57	28.39	31.42	33.93	33.20	29.15	42.10
Yb	2.59	2.50	2.18	2.43	2.42	2.24	2.30	2.56	2.84	2.89	2.48	3.74
Lu	0.37	0.36	0.32	0.35	0.35	0.32	0.32	0.37	0.40	0.42	0.35	0.55
Hf	4.75	4.71	4.99	5.35	5.47	4.89	5.12	4.89	5.44	5.59	4.87	6.33
Gd	6.41	6.45	6.13	6.95	6.79	6.93	6.44	6.23	6.50	6.95	6.44	8.16
Tb	1.03	1.07	1.00	1.09	1.05	1.03	0.98	1.00	1.04	1.11	0.97	1.27
Ho	1.15	1.13	0.99	1.10	1.11	1.06	1.01	1.14	1.23	1.25	1.11	1.49
Er	3.03	2.99	2.62	2.91	2.85	2.70	2.67	2.93	3.25	3.18	2.81	4.04
Li	58.66	107	73.58	51.86	52.92	65.80	47.98	46.72	121.55	35.42	28.43	59.62
Be	1.22	1.43	1.79	1.65	1.63	1.39	1.32	1.19	1.12	1.48	1.26	1.22
Sc	29.72	33.64	18.50	17.52	17.88	19.02	17.82	29.57	36.47	27.54	22.65	20.94
V	319	356	187	172	186	196	185	336	372	290	226	223
Cr	59.64	70.66	29.71	32.82	34.87	38.76	46.19	56.41	74.31	67.23	60.91	2.15
Co	44.53	52.46	44.13	48.87	55.14	52.07	58.27	48.41	50.70	52.37	47.82	37.63
Ni	54.34	60.19	55.77	84.59	91.77	89.14	114	59.92	64.66	78.80	135	37.44
Cu	98.44	99.83	39.14	52.17	52.85	51.98	51.41	89.76	57.72	277.58	497.62	11.04
Zn	540	515	471	142	144	136	142	130	221	170	143	853
Ga	21.62	24.35	23.13	21.80	23.09	21.01	20.83	21.67	25.96	23.89	23.30	22.33
Sn	1.54	1.64	1.84	1.99	1.83	1.82	1.76	1.52	1.94	1.80	1.78	1.94
Tm	0.41	0.42	0.36	0.39	0.38	0.36	0.35	0.40	0.45	0.45	0.39	0.57
Tl	0.06	0.06	0.10	0.11	0.06	0.09	0.14	0.18	0.23	0.05	0.03	0.03
Nb/Y	0.60	0.57	0.90	0.90	0.90	0.86	0.89	0.64	0.63	0.76	0.76	0.64
Lu/Yb	0.14	0.14	0.15	0.14	0.15	0.14	0.14	0.15	0.14	0.14	0.14	0.15
Ta/Th	0.51	0.52	0.64	0.66	0.62	0.74	0.65	0.55	0.53	0.70	0.64	0.65
La/Sm	3.79	3.50	3.77	3.69	3.70	3.77	3.77	3.85	2.97	3.69	3.48	3.79
Th/Nb	0.11	0.11	0.09	0.09	0.10	0.08	0.09	0.11	0.11	0.09	0.09	0.09
Nb/La	0.76	0.80	0.95	0.97	0.96	0.88	0.94	0.80	1.11	0.92	0.94	0.82

Bas MJ et al., 1986) to make related judgements has been inaccurate. In the Zr/TiO_2-Nb/Y diagram (Winchester JA and Floyd PA, 1977), given that the Nb/Y ratios range from 0.49 to 1.01, plotted of the five elements (Ti, P, Zr, Y, and Nb) in the mafic rocks at the boundary line between sub-alkaline basalts and alkali basalts (Fig. 6a) In the Nb/Y-Zr/(P_2O_5× 10000) diagram, they also plotted near the boundary line between alkali basalts and tholeiitic basalts (Fig. 6b). Therefore, the authors concluded that this is a transitional magmatic series.

4.2. Sr-Nd-Pb isotopic geochemistry

The Sr-Nd isotopic data for the samples in the Aksu mafic rocks are listed in Table 3. The results showed that the Sr-Nd isotopic characteristics of the mafic rock samples collected in

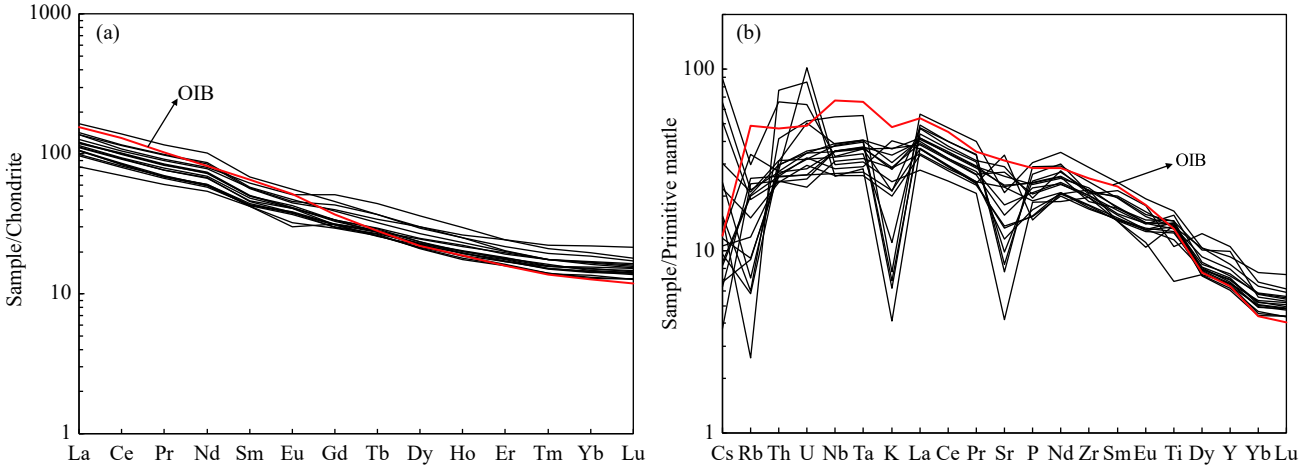

Fig. 5. Normalization plots. a–Chondrite-normalized REE patterns; b–primitive mantle-normalized multi-element diagrams of the mafic rocks in the Aksu. Chondrite and primitive mantle values are from Sun SS and McDonough WF (1989).

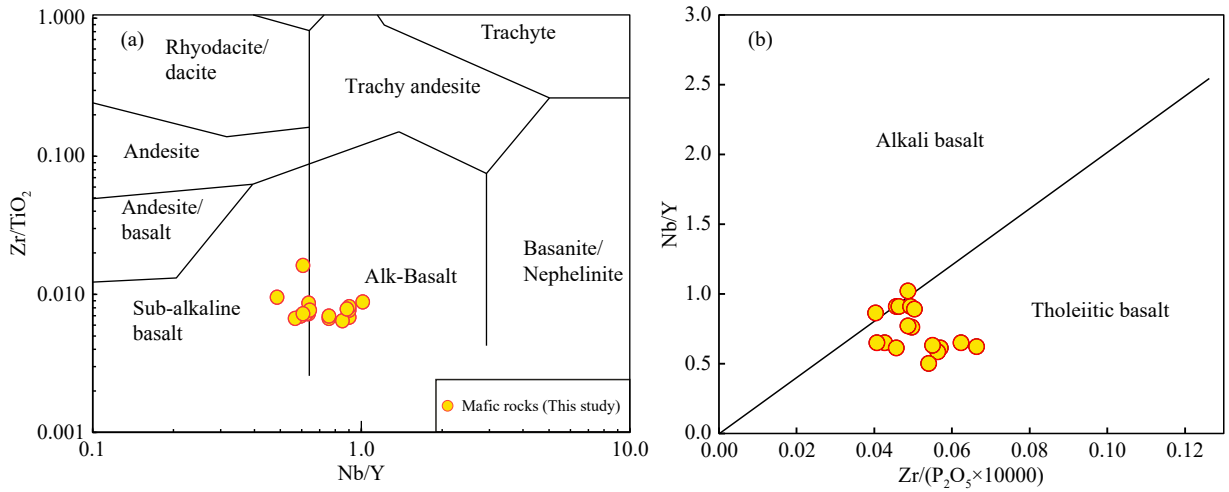

Fig. 6. Lithological classification diagrams of the mafic rocks in the Aksu. a–Zr/TiO_2-Nb/Y diagram (afterWinchester JA and Floyd PA, 1977); b–Nb/Y-$Zr/(P_2O_5\times10000)$ diagram (afterWinchester JA and Floyd PA, 1976).

the Aksu area were similar. The initial Sr and Nd isotopic ratios were corrected using the age of 615 Ma (Xu B et al. 2013 obtained the zircons from two samples of the Sugetbrak mafic rocks yield weighted mean ages of 615±4.8 Ma and 614.4±9.1 Ma). The mafic rock samples had initial $^{87}Sr/^{86}Sr$ (t=615 Ma) ratios ranging from 0.7052 to 0.7097. The $^{143}Nd/^{144}Nd$ values of the samples were similar (0.5121 to 0.5124), with $\varepsilon_{Nd}(t)$ values of –0.70 to –5.35. The Pb isotopic data of the rock samples are listed in Table 3. The samples exhibit concordant variations in Pb isotopic compositions, with $(^{206}Pb/^{204}Pb)_i$ of 16.9084 to 17.9817, $(^{207}Pb/^{204}Pb)_i$ of 15.4782 to 15.6273, and $(^{208}Pb/^{204}Pb)_i$ of 37.2760 to 38.6033.

5. Discussion

5.1. Magmatic consanguinity of the mafic rocks

In this paper, studies on mafic rocks in the Sugetbrak Formation in the Aksu area along three sections are presented. Whether the mafic rocks of the Sugetbrak Formation in this area are extrusive or intrusive is still controversial. On the basis of detailed fieldwork, the author observed phenomenon of the intruded strata in most layers of mafic rocks (Fig. 3), especially for the intruded upper strata, meanwhile, the red baked zone was observed at the contact boundary of overlying sandstone strata, the mafic rocks here have obvious phase transformation characteristics, and the crystalline particles of the mafic rocks near the formation contact boundary are very fine, while the mineral crystalline particles inside the mafic rocks become coarse, in other word, the crystal particles of the mafic rocks are transformed from marginal facies, transitional facies to mesophase facies. In addition to the above-mentioned macroscopic output characteristics, these mafic rocks are generally do not develop amygdaloidal structure and vesicular structure, with significant local spherical weathering, it is found that the mafic rocks have a typical diabasic structure and poikilophitic texture (Figs. 2e, f), These evidences strongly prove that these mafic rocks are actually formed by magma intrusion (Ren KX et al., 2009; Xiao YY et al., 2011; Lu YZ et al., 2018).

The Sugetbrak mafic rocks in the Aksu area are developed in similar spatial locations, basically belonging to the same

Table 3. Sr-Nd-Pb isotopic compositions of mafic rocks in the Aksu, NW Tarim Block.

Sample	20LKG-1-2	20LKG-2-1	20LKG-3	20LKG-4-1	20YRM-3-2	20YRM-2-2	20YRM-1-1	20YRM-1-3
Rb/$\times10^{-6}$	9.69	21.5	13.4	12.2	14.9	5.82	1.64	4.49
Sr/$\times10^{-6}$	289.55	331.65	542.96	486.80	472.57	178.61	245.93	207.89
$^{87}Rb/^{86}Sr$	0.094	0.183	0.069	0.071	0.089	0.092	0.019	0.061
$^{87}Sr/^{86}Sr$	0.706577	0.710175	0.706860	0.707487	0.705960	0.710225	0.709817	0.709139
$(^{87}Sr/^{86}Sr)i$	0.705749	0.708569	0.706251	0.706865	0.705181	0.709419	0.709652	0.708604
Sm(ppm)	6.60	6.98	7.63	7.61	6.73	8.90	6.45	8.76
Nd(ppm)	27.13	31.56	33.95	34.39	28.38	40.71	27.81	36.62
$^{147}Sm/^{144}Nd$	0.1534	0.1394	0.1417	0.1395	0.1495	0.1378	0.1463	0.1508
$^{143}Nd/^{144}Nd$	0.512384	0.512354	0.512339	0.512334	0.512412	0.512127	0.512173	0.512305
$\varepsilon Nd(t)$	−1.55	−1.0	−1.5	−1.4	−0.7	−5.35	−5.11	−2.89
$^{206}Pb/^{204}Pb$	16.9890	17.0100	17.6128	17.9422	18.4766	17.5791	19.2960	17.8263
$^{207}Pb/^{204}Pb$	15.4783	15.4780	15.4818	15.5260	15.6597	15.5128	15.7210	15.5716
$^{208}Pb/^{204}Pb$	37.4238	37.4386	38.1486	38.5041	39.1985	38.1213	40.0849	38.4060
$(^{206}Pb/^{204}Pb)i$	16.9875	16.9848	16.9084	17.3591	17.9396	17.1739	17.9817	17.7685
$(^{207}Pb/^{204}Pb)i$	15.4782	15.4765	15.4393	15.4908	15.6273	15.4884	15.6417	15.5681
$(^{208}Pb/^{204}Pb)i$	37.4223	37.4135	37.2760	37.7961	38.4697	37.7022	38.6033	38.3615

Note: $(^{147}Sm/^{144}Nd)_{CHUR}$=0.1967, $(^{143}Nd/^{144}Nd)_{CHUR}$=0.512638 (Hamilton PJ et al., 1983);$(^{147}Sm/^{144}Nd)_{DM}$=0.2137, $(^{143}Nd/^{144}Nd)_{DM}$=0.51315(Goldstein SL et al., 1984); $\lambda_{Rb}=1.42\times10^{-11}$ year^{-1}, $\lambda_{Sm}=6.54\times10^{-12}$ year^{-1} (Lugmair GW et al., 1978). $\lambda_{U238}=1.55125\times10^{-10}$ year^{-1}, $\lambda_{U235}=9.8485\times10^{-10}$ year^{-1}, $\lambda_{Th232}=4.9475\times10^{-11}$ year^{-1} (Steiger RH and Jäger E, 1977).

tectonic setting, with similar geological characteristics in the field. Generally, the mafic rocks are developed in different layers in the Sugetbrak Formation. In addition, the mafic rocks have different degrees of invasion of the upper and lower sandstone layers. Further research show that these mafic rocks have similar petrographic characteristics and mineral composition. The mineral composition is mainly plagioclase (45%–50%), pyroxene (45%–50%) and Fe-Ti oxides (5%) and most of them have suffered slight alteration, and their main structure is diabasic structure and poikilophitic texture. The geochemical characteristics of the mafic rocks are basically similar. In the chondrite-normalized REE patterns and the primitive mantle-normalized spidergram, all the samples display similar elemental characteristics. In the Harker diagrams, the Sugetbrak mafic rocks exhibit strong correlations (Fig. 5), meanwhile, the mafic rocks of the three typical sections have generally similar initial values of Si-Nd-Pb isotopes, further confirming their genetic correlation. Based on the geology, petrology, element geochemistry and isotope geochemistry characteristics of the above the mafic rocks in the Sugetbrak Formation, the authors infer that the mafic rocks distributed in different sections of the Aksu area have a common mantle source.

5.2. Age assessment of the mafic rocks

Abundant mafic rocks crop out in different lithological section of the Aksu-Wushi and Yuermeinark areas. According to the regional stratigraphic research, many researchers have carried out detailed chronological studies on these mafic rocks. Wang F et al. (2010) used the LA-ICPMS U-Pb dating on the zircons from the mafic rocks in the Dongergou section which yielded ages ranging from 1945 Ma to 755 Ma (17 zircon analyses), indicating that these zircons were inherited from the crustal materials during the ascending of the magma. Thus, the ages of the mafic rocks are therefore considered to be younger than 755 Ma. Besides, Zhang ZC et al. (2012) reported a LA-MC-ICP-MS U-Pb zircon age of 783.7 ± 2.3 Ma (23 zircon analyses) form the upper mafic rocks in the south of Yuermeinark section, these radiometric dates suggested it as the crystallization age of the mafic rocks in the Sugetbbrak Fomation, however, this result was inconsistent with the fact that the strata belonged to the Ediacaran. According to previous reports (Gao Z et al., 1985), the Chigebrak Formation, overlaying the Sugetbrak Formation, developed a large number of Ediacaran indicative stromatolite assemblages, therefore the Chigebrak Formation and the Sugetbrak Formation were jointly classified as the Ediacaran. Furthermore, these ages are even older than the metamorphic age of the underlying Aksu Group (Liou JG et al., 1996; Wen B et al., 2015). Recently, Lu YZ et al. (2018) studied the geochronology of the mafic rocks in the Aksu area again, and he performed $^{40}Ar/^{39}Ar$ analyses on the plagioclase and pyroxene from most layer of the mafic rocks the Sugetbrak Formation yield, due to the alteration of sericitization in the plagioclases, the $^{40}Ar/^{39}Ar$ age of plagioclase was not obtained, and the $^{40}Ar/^{39}Ar$ plateau age of 521.0 ± 2.1 Ma and the mini--inverse isochron age of 520.6 ± 2.1 Ma were obtained only from a pyroxene mineral. Since the two results are consistent, it can be concluded that there is no excess Ar in pyroxenes. However, it should be noted that pyroxene is a mineral with very low potassium content, so it is usually difficult to obtain reliable $^{40}Ar/^{39}Ar$ age results. Moreover, according to detailed microscope observation, the pyroxene in the mafic rocks in the study area had undergone relatively weak alteration. Additionally, since the $^{40}Ar/^{39}Ar$ age results of pyroxene indicated the Cambrian, according to the stratigraphic records of Cambrian in Tarim Block, there is no

record of magmatism in the regional strata of Cambrian, so whether this result can be recognized as the diagenetic age of the mafic rocks is still questionable. Xu B et al. (2013) reported a U-Pb zircon age of 615.2 ± 4.8 Ma and 614.4 ± 9.1 Ma providing an age constraint on the timing of the Sugetbrak Formation. Based on the stratigraphic relationship with the Chigebrak dolomite, the Chigebrak Formation and the Sugetbulak Formation are collectively classified into the Ediacaran Formation, moreover, the presence of 615 ± 15 Ma volcanic rocks in the Mochia-Khutuk area of the northeast Tarim Block (Xu B et al., 2009), and 588–619 Ma detrital zircons in the Aksu area of the northwest Tarim Block (Zhu WB et al., 2011), Xu B et al. (2013) reported this age of 615 Ma correspond to them in time. To sum up, the author infered that the age of 615 Ma may be the most reliable age of the mafic rocks in the Sugetbrak Formation in the Aksu area.

5.3. Nature of the mantle source

The presence of voluminous phenocrysts (clinopyroxene and plagioclase) in the mafic rocks, suggesting fractional crystallization of clinopyroxene and plagioclase (Frey FA and Prinz M, 1978). The Aksu Sugetebrak Formation mafic rocks showed low MgO contents (3.52%–7.88%) and $Mg^{\#}$ (34–51) as well as relatively low contents of compatible elements, such as Ni (19×10^{-6}–136×10^{-6}) and Cr (1.4×10^{-6}–74×10^{-6}). The correlation of Ni, Cr, and CaO/Al_2O_3 with $Mg^{\#}$ in these mafic rocks indicated in the early crystallization of olivine and clinopyroxene, respectively (Figs. 7a, b). The petrological and geochemical characteristics indicated that they represent evolved magmas rather than primary magmas.

Most of the samples showed Ba contents of 110×10^{-6}–1483×10^{-6} and Sr contents of 85.8×10^{-6}–711×10^{-6}, much higher than those of the primitive mantle on average (Ba = 5.1×10^{-6}, Sr = 19.9×10^{-6}; Taylor SR and McLennan S, 1995), which indicated that the magma source of the mafic rocks involved some crustal materials. In the process of fractional crystallization, the incompatible elements are relatively enriched in the residual melt, while the Sr-Nd-Pb isotope is not affected. Therefore, their relatively high $(^{87}Sr/^{86}Sr)_i$ ratios (0.7052–0.7097), negative $\varepsilon_{Nd}(t)$ values of (–0.70 to –5.35) and high $(^{206}Pb/^{204}Pb)_i$ ratios (16.9084–17.9817) implied the involvement of crustal materials which were enriched in these isotope ratios. Crustal materials can incorporate in the formation of these mafic rocks via two ways, i.e., the crust contamination and source enrichment.

Mantle-sourced magma may be affected by crustal contamination as it rises or temporarily settles in magma chambers in the continental crust. Some incompatible elements have similar geochemical characters, such as Ta and Th, La and Sm, hence Ta/Th and La/Sm ratios cannot be significantly modified by partial melting or fractional crystallization. Mantle-derived magmas are characterized by low La/Sm ratios and high Ta/Th (Sun SS and McDonough WF, 1989). The Ta/Th *vs*. La/Sm diagram (Fig. 8) showed that the Sugetbrak mafic rocks plotted between upper crust and OIB, suggesting some crustal contamination. However, the Lu/Yb value of the characteristic rock of mantle-derived magma (0.14–0.15) was low (Sun SS and McDonough WF, 1989); this was consistent with the results obtained for the Sugetbrak mafic rocks (0.14–0.15). In chondrite-normalized REE patterns and primitive mantle normalized spidergrams, the lack of negative Eu and Ti anomalies also argued against the possibility of extensive crustal contamination (Rudnick R and Gao S, 2003). Meanwhile, the Nb and Ta contents in the samples showed no obvious depletion, and most of the Sugetbrak samples had chondritic Nb/Ta (16–17), Zr/Hf (40–45) and Nb/U (30–47) ratios, which suggested that crustal contamination had less effect in magma source (Sun SS and McDonough WF, 1989). Moreover, In the SiO_2 *vs*. initial Sr isotopic ratio and $\varepsilon_{Nd}(t)$ diagram (Fig. 9), the Sugetbrak mafic rocks exhibit no correlations between $(^{87}Sr/^{86}Sr)_i$ *vs*. SiO_2 and between $\varepsilon_{Nd}(t)$ *vs*. SiO_2. All these above demonstrated that the magma was not significantly affected by crustal contamination during their ascent to the continental crust. In summary, all the evidence suggests that the parental magma of the Neoproterozoic mafic rocks in the Aksu experienced slight crustal contamination as it ascended the surface.

As discussed above, the Sugetbrak mafic rocks had undergone insignificant crustal contamination, the crustal

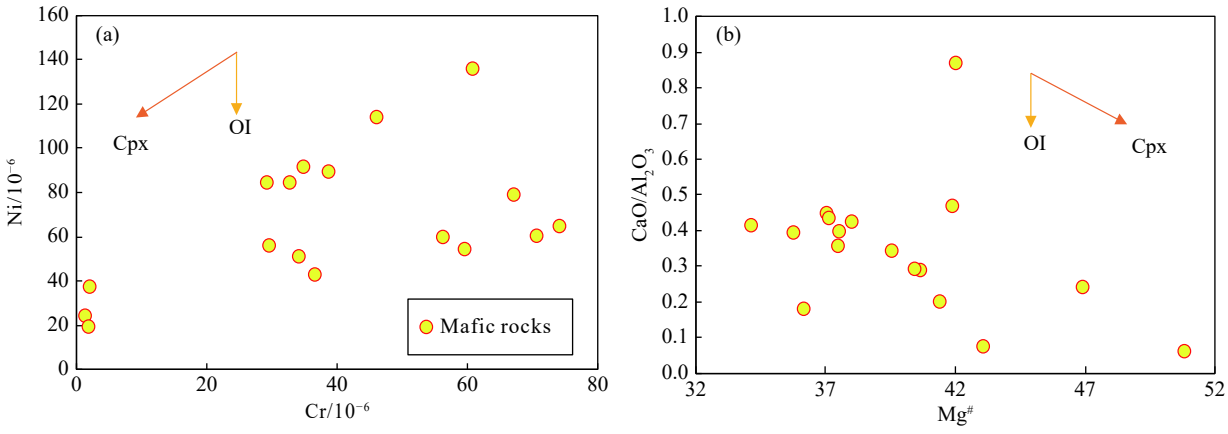

Fig. 7. Elemental variation diagrams of the mafic rocks in the Aksu. a–Ni *vs*. Cr diagram; b–CaO/Al_2O_3 *vs*. $Mg^{\#}$ diagram. Arrows showing fractional crystallization trends in the evolution of the mafic rocks in the Aksu. Partition coefficients are from Rollision HR (1993). Arrows in the diagrams indicate data trends. Cpx: clinopyroxene; Ol: olivine.

materials might have been involved in the source region. In the $^{87}Sr/^{86}Sr$ *vs.* $^{206}Pb/^{204}Pb$ isotope correlation diagram and the $\varepsilon_{Nd}(t)$ *vs.* $^{206}Pb/^{204}Pb$ isotope diagram, most of the sample plots were observed near EM-Ⅰ (Figs. 10a, b), Additionally, Pb isotope source discriminant diagram (Fig. 11) show that the data of Sugetbrak mafic rocks plotted near the lower crust, combining to eliminate the influence of crustal contamination, indicating that the magma of the mafic rocks might be derived from a relatively enriched mantle with some lower crustal materials involved.

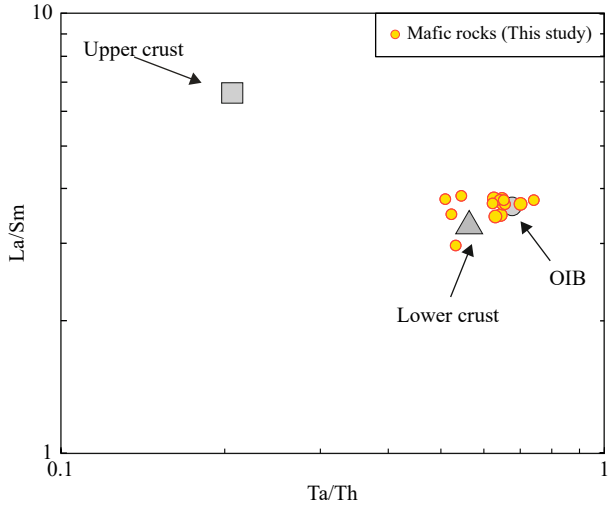

Fig. 8. Ta/Th *vs.* La/Sm diagram of the Sugetbrak mafic rocks. OIB data from Sun SS and McDonough WF (1989), and upper crust and lower crust data from Taylor SR and McLennan S (1995).

In the diagram of $(^{87}Sr/^{86}Sr)_t$ *vs.* $\varepsilon_{Nd}(t)$, most samples were close to the OIB field (Fig. 6), meanwhile, the trace element characteristics of the samples were roughly similar to those of the OIB-like trace element patterns and REE patterns characterized by enrichment of large-ion lithophile elements (LILE), high field strength elements (HFSE), and LREE with no significant negative Nb or Ta anomalies, typical of OIB. It may indicate that the source region has received metasomatism of recycled materials.

5.4. Tectonic implications

Ti, Zr, Y, and Nb are immobile trace elements during the metamorphic process of the zeolite to greenschist facies and can be used to determine the tectonic environment of mafic rocks (Pearce JA and Cann JR, 1973; Winchester JA and

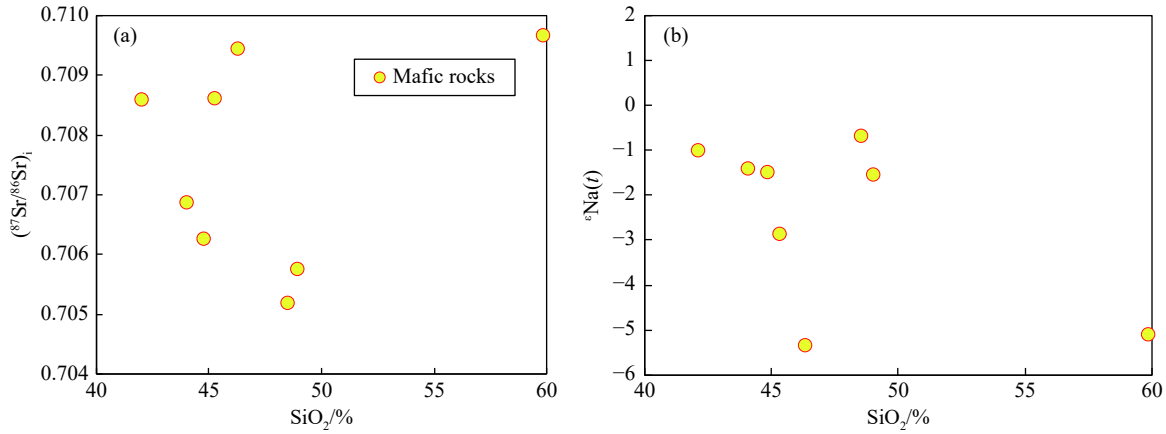

Fig. 9. SiO_2 *vs.* Sr-Nd isotopic ratios. a–SiO_2 *vs.* $(^{87}Sr/^{86}Sr)_i$, b–SiO_2 vs. $\varepsilon_{Nd}(t)$ diagrams. All mafic rocks exhibit not correlation between $(^{87}Sr/^{86}Sr)_i$ and SiO_2 and between $\varepsilon_{Nd}(t)$ and SiO_2.

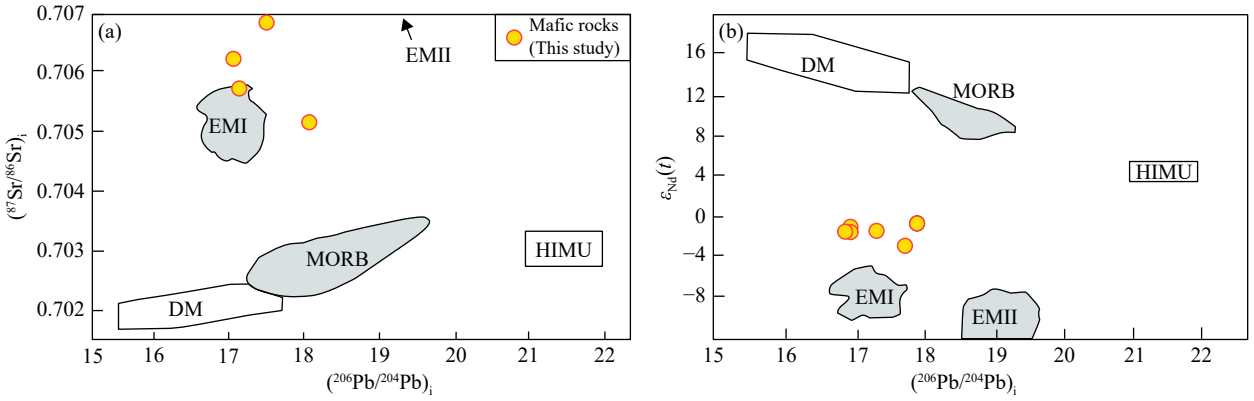

Fig. 10. Source divisional diagrams of Sr-Nd isotope of mafic rocks in the Aksu. a–$^{87}Sr/^{86}Sr$ *vs.* $^{206}Pb/^{204}Pb$ isotope correlation diagram; b–$\varepsilon_{Nd}(t)$ *vs.* $^{206}Pb/^{204}Pb$ isotope correlation diagram. Both diagrams show the positions of the mantle reservoirs identified by Zindle A and Hart SR (1986): DM, depleted mantle; HIMU, mantle with high U/Pb ratio; EM Ⅰ and EM Ⅱ, enriched mantle sources; MORB, mid-ocean ridge basalt (after Zindle A and Hart SR, 1986). Fields of MORB, EMI and EMII with shadow-hatching. In above figures all Pb isotopes plotting are the measured value.

Floyd PA, 1976). In the Zr/4-Nb×2-Y triangle diagram (Meschede M, 1986), all the sample input points were within the areas of intra-plate alkali basalt and intra-plate tholeiite, meanwhile, in the Zr/Y-Zr diagram (Pearce JA and Norry MJ, 1979), all the samples plotted in the field of intraplate tectonic setting. (Figs. 12a, b). Both Zr/4-Nb×2-Y and Zr/Y-Zr diagrams suggested the intra-plate environment.

Neoproterozoic magmatic records have been reported in the Tarim Block (Li ZX et al., 1999; Xu B et al., 2005; Zhang ZC et al., 2009, 2012). Four stages of Neoproterozoic magmatic events have been reported in the Tarim Block: 820–800 Ma, 780–760 Ma, 740–735 Ma and 650–635 Ma (Li XH et al., 2003; Li ZX et al., 1996, 2003, 2008; Zhang CL et al., 2011; Zhang ZC et al., 2012), including the age of bimodal volcanic rocks from the Beiyixi Formation of the Quruqtagh area was 755 ± 15 Ma (Xu B et al., 2005) and that of the volcanic agglomerate from the Beiyixi Formation was 739±6 Ma (Gao Z et al., 2010); the basalt age in the Beiyixi Formation was 740±7 Ma and 725±10 Ma, while the andesite age was 615±6 Ma in the Zhamokti Formation (Xu B et al., 2009). Recently, some scholars have proposed that the mafic rocks of the Sugetebrak Formation are caused by the mantle plume activity under the Neoproterozoic Rodinia supercontinent and are evidence of the pyrolysis of the Tarim plate from the Rodinia supercontinent (Wang F et al., 2010). Xu B et al. (2013) evaluated the zircon age of the Sugetebrak Formation; the youngest rocks exhibited an age of 615 Ma, this age interpreted as the eruption of the Sugetbrak mafic rocks Furthermore, the Sugetebrak mafic rocks were associated with a plume-related magmatism during the Neoproterozoic may represent the waning stage of plum volcanism during a long-lasting continental breakup. Previous studies have shown that the Sugetbrak Formation in the southwest Aksu areas has been interpreted as fluvial and lacustrine facies sediments (Turner S, 2010, Wang F et al., 2010). Combined with several horizons of mafic rocks that record episodic volcanism, these sedimentary facies are thought to indicate the development of a Neoproterozoic rift system the Aksu area. In our research, the Sugetbrak mafic rocks belong to intra-plate environment, so it suggests that the Sugetbrak mafic rocks may represent the last stage of the Neoproterozoic rifting associated with the breakup of the

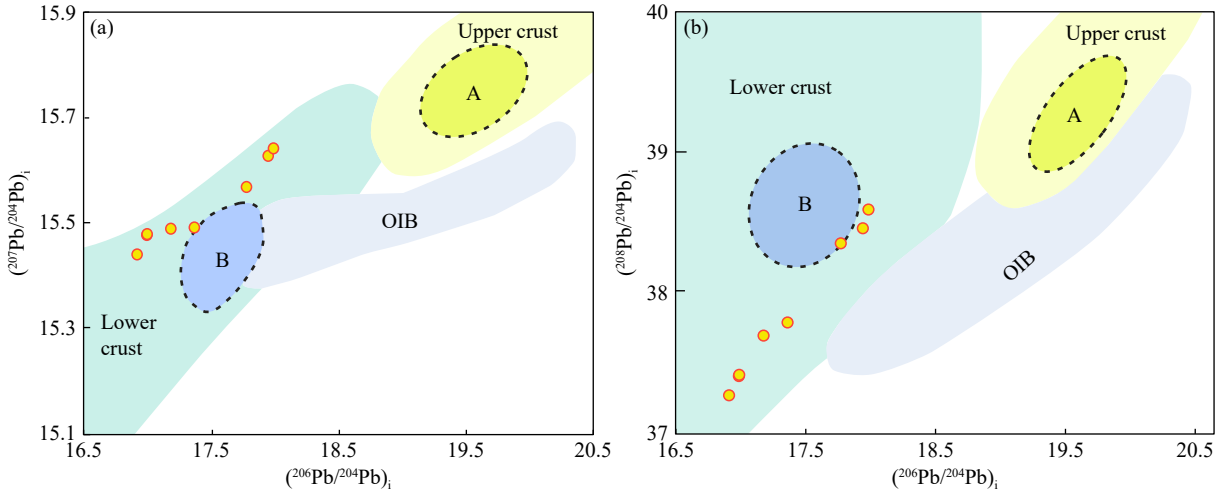

Fig. 11. Source divisional diagram of Pb isotope in the Sugetbrak mafic rocks. Dashed lines enclose probable average values (a–upper crust; b–lower crust; base map after Doe BR and Zartman RE, 1979) .

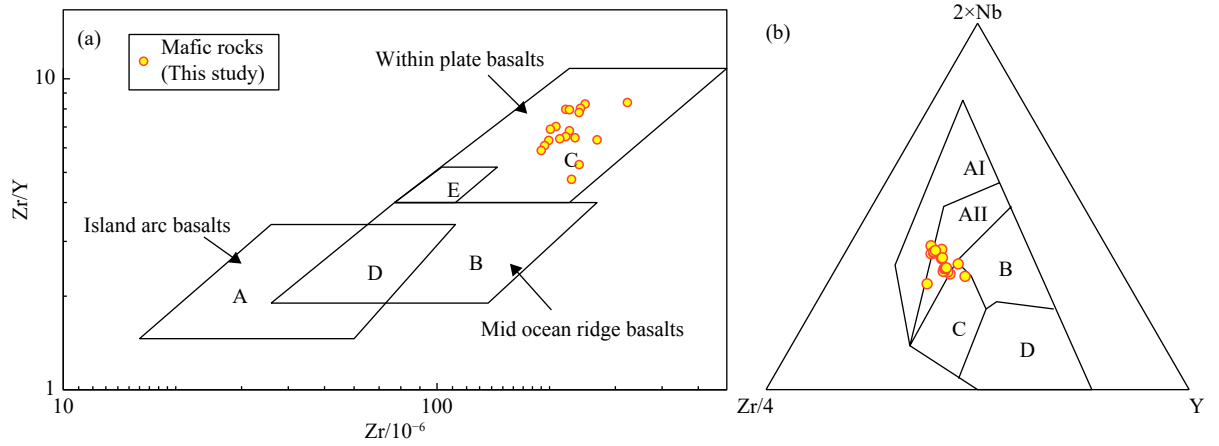

Fig. 12. Tectonic discrimination diagrams of mafic dikes in the Aksu. a–The Zr/Y *vs*. Zr diagram (after Pearce JA and Norry MJ, 1979); A–Island arc basalts; B–Mid ocean ridge basalts; C–Within plate basalts. b–the Nb-Zr-Y diagram (after Meschede M, 1986). A Ⅰ +A Ⅱ – Intra-plate alkaline basalts; (A Ⅱ +C)–Intra-plate tholeiite; B–P-Mid ocean ridge basalts; (C+D)–Volcanic arc basalts; D–N-Mid ocean ridge basalts.

Rodinia Supercontinent.

6. Conclusions

Based on the petrological, geochemical and Sr-Nd-Pb isotopic studies of the mafic rocks in the Aksu area of the northwest Tarim block, the author made several conclusions:

(i) Based on the similar geological, petrological, element geochemical and isotope geochemical characteristics of the mafic rocks in the Sugetbrak Formation, the author infer that these mafic rocks distributed in different sections of the Aksu area have a common mantle source.

(ii) Petrological and geochemical characteristics indicated that the Sugetbrak mafic rocks in the Aksu represent evolved magmas rather than primary magmas, and they had not undergone significant crustal contamination during ascent to the surface, most of the sample plots were observed near EM-Ⅰ, indicating that the magma of the mafic rocks might be derived from a relatively enriched mantle with some crustal materials involved. They showed OIB-like geochemical characteristics indicating that the source region has experienced metasomatism of recycled materials.

(iii) The mafic rocks of the Sugetbrak Formation in the Aksu area were formed in an intraplate rift environment, which might result from the breakup of the Rodinia supercontinent and represent the waning stage of plume volcanism during a long-lasting continental breakup.

CRediT authorship contribution statement

Xiang-kun Zhu conceived of the presented idea. Hong-zhe Xie, Xun Wang, Yuan He, Wei-bing Shen wrote the manuscript in consultation. All authors discussed the results and contributed to the final manuscript.

Declaration of competing interest

The authors declare no conflicts of interest.

Acknowledgement

This work was funded by the Key Laboratory of Deep-Earth Dynamics of Ministry of Natural Resources (J1901-20-1), and China Geological Survey Program (D20090002). The authors are grateful to Dr. Zhao-fu Gao and Dr. Qiu-hong Xie and three anonymous reviewers for their constructive comments and suggestions which substantially improved this work in science and presentation.

References

Baker J, Peate D, Waight T, Meyzen C. 2004. Pb isotopic analysis of standards and samples using a ^{207}Pb-^{204}Pb double spike and thallium to correct for mass bias with a double-focusing MC-ICP-MS. Chemical Geology, 211(3 –4), 275 –303. doi: 10.1016/j.chemgeo.2004.06.030

Chen Y, Xu B, Zhan S, Li Y. 2004. First Mid-Neoproterozoic paleomagnetic results from the Tarim Basin (NW China) and their geodynamic implications. Precambrian Research, 133, 271–281. doi: 10.1016/j.precamres.2004.05.002.

Ding HF., Ma DS, Lin QZ, Jing LH. 2015. Age and nature of Cryogenian diamictites at Aksu, Northwest China: Implications for Sturtian tectonics and climate. International Geology Review, 57, 2044–2064. doi: 10.1080/00206814.2015.1050463.

Direen N, Crawford A. 2003. Fossil seaward-dipping reflector sequences preserved in southeastern Australia: A 600 Ma volcanic passive margin in eastern Gondwanaland. Journal of the Geological Society, London 160, 985–990. doi: 10.1144/0016-764903-010

Doe BR and Zartman RE. 1979. Plumbotectonics: The Phanerozoic. In:Barnes HL (ed.). Geochemistry of Hydrothermal Ore Deposit. 2nd Edition. New York:Wiley Interscience, 22–70.

Frey FA, Prinz M. 1978. Ultramafic inclusions from San Carlos, Arizona: Petrologic and geochemical data bearing on their petrogenesis. Earth and Planetary Science Letters, 38, 129–176. doi: 10.1016/0012-821X(78)90130-9.

Gao LZ, Wang ZQ, Xu ZQ, Yang JS, Zhang W. 2010. A new evidence from zircon SHRIMP U-Pb dating of the Neoproterozoic diamictite in Quruqtagh area, Tarim basin, Xinjiang, China. Geological Bulletin of China, 29(2/3), 205–213 (in Chinese with English abstract). doi: 10.1017/S0004972710001772.

Gao Z, Qian J. 1985. Sinian glacial deposits in Xinjiang, Northwest China. Precambrian Research, 29, 143–147. doi: 10.1016/0301-9268(85)90065-8.

Gao Z, Wang W, Peng C, Li Y, Xiao B. 1986. The Sinian System on Aksu-Wushi Region, Xinjiang. Urumqi. Xinjiang People 's Publishing House, 1–184 (in Chinese with English abstract).

Goldstein SL, O'Nion RK, Hamilton PJ. 1984. A Sm-Nd isotopic study of atmospheric dusts and particulates from major river system. Earth and Planetary Science Letters, 70, 221–236. doi: 10.1016/0012-821X(84)90007-4.

Hamilton PJ, O 'Nions RK, Bridgwater D, Nutman A. 1983. Sm-Nd studies of Archaean metasediments and metavolcanics from West Greenland and their implications for the Earth's early history. Earth and Planetary Science Letters, 62, 263–272. doi: 10.1016/0012-821X(83)90089-4.

He JY, Xu B, Li D. 2019. Newly discovered early Neoproterozoic (ca. 900 Ma) andesitic rocks in the northwestern Tarim Craton: Implications for the reconstruction of the Rodinia supercontinent. Precambrian Research, 325, 55–68. doi: 10.1016/j.precamres.2019.02.018

Karlstrom KE, Bowring SA, Dehler CM, Knoll AH, Porter SM, Marais DJDB, Weil A, Sharp ZD, Geissman JW, Elrick MB, Timmons JM, Crossey LJ, Davidek KL. 2000. Chuar group of the grand canyon: Record of breakup of Rodinia, associated change in the global carbon cycle, and ecosystem expansion by 740 Ma. Geology, 28, 619–622. doi: 10.1130/0091-7613(2000)282.0.CO;2.

Le Bas MJ, Le Maitre RW, Streckeisen A, Zanettin B. 1986. A chemical classification of volcanic rocks based on the total alkali-silica diagram. Journal of Petrology, 27, 745–750. doi: 10.1093/petrology/27.3.745.

Li CF, Li XH, Li QL, Guo JH, Yang YH. 2012. Rapid and precise determination of Sr and Nd isotopic ratios in geological samples from the same filament loading by thermal ionization mass spectrometry employing a single-step separation scheme. Analytica Chimica Acta, 727(10), 54–60. doi: 10.1016/j.aca.2012.03.040.

Li XH, Li ZX, Ge W, Zhou H, Li W, Liu Y, Wingate MTD. 2003. Neoproterozoic granitoids in South China: crustal melting above a mantle plume at ca. 825 Ma? Precambrian Research, 122, 45–84. doi: 10.1016/S0301-9268(02)00207-3.

Li XH, Li ZX, Wingate MTD, Chung SL, Liu Y, Lin GC, Li WX. 2006. Geochemistry of the 755 Ma Mundine Well dyke swarm, northwestern Australia: Part of a Neoproterozoic mantle superplume beneath Rodinia? Precambrian Research, 146, 1 –15. doi: 10.1016/j.precamres.2005.12.007

Li ZX, Bogdanova SV, Collins AS, Davidson A, De Waele B, Ernst RE, Fitzsimons ICW, Fuck RA, Gladkochub DP, Jacobs J, Karlstrom KE, Lu S, Natapov LM, Pease V, Pisarevsky SA, Thrane K, Vernikovsky V. 2008. Assembly, configuration, and break-up history of Rodinia: A synthesis. Precambrian Research, 160, 179–210. doi: 10.1016/j.precamres.2007.04.021.

Li ZX, Li XH, Kinny PD, Wang J. 1999. The breakup of Rodinia: Did it start with a mantle plume beneath South China? Earth and Planetary Science Letters, 173, 171–181. doi: 10.1016/S0012-821X(99)00240-X.

Li ZX, Li XH, Kinny PD, Wang J, Zhang S, Zhou H. 2003. Geochronology of Neoproterozoic syn-rift magmatism in the Yangtze Craton, South China and correlations with other continents: Evidence for a mantle superplume that broke up Rodinia. Precambian Research, 122, 85–110. doi: 10.1016/S0301-9268(02)00208-5.

Li ZX, Powell CM. 2001. An outline of the palaeogeographic evolution of the Australasian region since the beginning of the Neoproterozoic. Earth Science Reviews, 53, 237–277. doi: 10.1016/S0012-8252(00)00021-0.

Li ZX, Zhang L, Powell CM. 1996. Positions of the East Asian cratons in the Neoproterozoic supercontinent Rodinia. Australian Journal of Earth Sciences, 43, 593–604. doi: 10.1080/08120099608728281.

Liou JG, Graham SA, Maruyama S, Zhang RY. 1996. Characteristics and tectonicsignificance of the late Proterozoic Aksu blueschists and diabasic dikes, Northwest Xinjiang, China. International Geological Review, 38, 228–244. doi: 10.1080/00206819709465332.

Liou JG, Graham SA, Mayuyama S, Wang X, Xiao X, Carrroll AR, Chu J, Feng Y, Hendrix MS, Liang Y, Mcknight CL, Yang Y, Wang Z, Zhao M, Zhu B. 1989. Proterozoic blueschistbelt in westernChina: Best-documented precambrian blueschists in the world. Geology, 17, 1127–1131. doi: 10.1130/0091-7613(1989)017<1127:PBBIWC>2.3.CO;2.

Lu YZ, Zhu WB, Ge RF, Zheng BH, He JW, Diao Z. 2017. Neoproterozoic active continental margin in the northwestern Tarim Craton: Clues from Neoproterozoic (meta) sedimentary rocks in the Wushi area, northwest China. Precambrian Research, 88–106. doi: 1016/j.precamres.2017.06.002.

Lu YZ, Zhu W, Jourdan F. 2018. $^{40}Ar/^{39}Ar$ ages and geological significance of Neoproterozoic-Cambrian mafic rocks in the Aksu-Wushi area, NW Tarim Craton. Geological Journal, 54(6), 3803–3820. doi: 10.1002/gj.3375.

Lugmair GW, Harti K. 1978. Lunar initial $^{143}Nd/^{144}Nd$: differential evolution of the lunar crust and mantle. Earth and Planetary Science Letters, 39, 349–357. doi: 10.1016/0012-821X(78)90021-3.

Meschede M. 1986. A method of discriminating between different types of micocean ridge basalts and continental tholeiites with the Nb–Zr–Y diagram. Chemical Geology, 56, 207–218. doi: 10.1016/0009-2541(86)90004-5.

Nakajima T, Maruyama S, Uchiumi S, Liou JG, Wang X, Xiao X, Graham A. 1990. Evidence for late Proterozoic subduction from 700-My-old blueschists in China. Nature, 346, 263–265. doi: 10.1038/346263a0.

Pearce JA, Cann JR. 1973. Tectonic setting of basic volcanic rocks determined using trace element analyses. Earth and Planetary Science Letters, 19.2, 290–300. doi: 10.1016/0012-821X(73)90129-5.

Pearce JA, Norry MJ. 1979. Petrogenetic implications of Ti, Zr, Y, and Nb variations in volcanic rocks. Contributions to Mineralogy and Petrology, 69(1), 33–47. doi: 10.1007/BF00375192.

Ren KX, Zheng Y, Xia Z. 2009, Characteristics of igneous rocks of upper Sinian section in Xiaoerbulake of Aksu, Xinjiang. Xinjiang Petroleum Geology, 30(01), 51 –52. (in Chinese with English abstract). doi: 1016/S1874-8651(10)60080-4

Rollinson HR. 1993. Using Geochemical Data: Evaluation, Presentation, Interpretation. Longman Singapore Publishers Ltd., Singapore, 1–351.

Rudnick R, Gao S. 2003. Composition of the continental crust. In: Rudnick, R. L. (Ed.), Treatise on Geochemistry, vol. 3. Elsevier-Pergamon, Oxford, 1–64. doi: 10.1016/B978-0-08-095975-7.00301-6ù

Steiger RH, Jäger E. 1977. Subcommission on geochronology: convention on the use of decay constants in geology and cosmochronology. Earth and Planetary Science Letters 36, 359–362. doi: 10.1016/0012-821X(77)90060-7.

Sun SS, McDonough WF. 1989. Chemical and isotopic systematics of oceanic basalts: Implications for mantle composition and processes. In: Saunders, A. D. , Norry, M. J. (Eds.), Magmatism in the Ocean Basins, Special Publications 42. Geological Society, London, 313–345. doi: 10.1144/GSL.SP.1989.042.01.19

Tanaka T, Togashi S, Kamioka H, Amakawa H, Kagami H, Hamamoto T, Yuhara M, Orihashi Y, Yoneda S, Shimizu H, Kunimaru T, Takahashi K, Yanagi T, Nakano T, Fujimaki H, Shinjo R, Asahara Y, Tanimizu M, Dragusanu C. 2000. Jndi-1: a neodymium isotopic reference in consistency with lajolla neodymium. Chemical Geology, 168(168), 279–281. doi: 10.1016/S0009-2541(00)00198-4.

Taylor SR, McLennan S. 1995. The geochemical evolution of the continental crust. Review in Geophysics, 33, 241–265. doi: 10.1029/95RG00262.

Thirlwall MF. 1991. Long–term reproducibility of multicollector sr and nd isotope ratio analysis. Chemical Geology, 94(2), 85–104. doi: 10.1016/S0009-2541(10)80021-X.

Turner S. 2010. Sedimentary record of Late Neoproterozoic rifting in the NW Tarim basin, China. Precambrian Research, 181, 85–96. doi: 10.1016/j.precamres.2010.05.015.

Veevers JJ, Walter MR, Scheibner E. 1997. Neoproterozoic tectonics of Australia-Antarctica and Laurentia and the 560 Ma birth of the Pacific ocean reflect the 400 m. y. Pangean supercycle. The Journal of Geology, 105, 225–242. doi: 10.1086/515914.

Wang F, Wang B, Shu LS. 2010. Continental tholeiitic basalt of the Akesu area (NW China) and its implication for Neoproterozoic rifting in the northern Tarim. Acta Petrologica Sinica, 26, 547–558 (in Chinese with English abstract).

Wen B, David AD Evans, Li YX, Wang ZR, Liu C. 2015. Newly discovered Neoproterozoic diamictite and cap carbonate (DCC) couplet in Tarim Craton, NW China: Stratigraphy, geochemistry, and paleoenvironment. Precambrian Research, 271, 278–294. doi: 10.1016/j.precamres.2015.10.006.

Winchester JA, Floyd PA. 1976. Geochemical magma type discrimination: Application to altered and metamorphosed igneous rocks. Earth and Planetary Science Letters, 28, 459–469. doi: 10.1016/0012-821X(76)90207-7.

Winchester JA, Floyd PA. 1977. Geochemical discrimination of different magma series and their differentiation products using immobile elements. Chemical Geology, 20, 325–343. doi: 10.1016/0009-2541(77)90057-2.

Wingate MTD, Campbell IH, Compston W, Gibson GM. 1998. Ion microprobe U-Pb ages for Neoproterozoic basaltic magmatism in south-central Australia and implications for the breakup of Rodinia. Precambrian Research, 87, 135–159. doi: 10.1016/S0301-9268(97)00072-7.

XBGMR (1957–1961). 1: 200000 Geological map of RPC, Wushi sheet (K-46-XXVI)National 543 Publishing House. (in Chinese).

Xia B, Zhang LF, Du ZX, Xu B. 2017. Petrology and age of Precambrian Aksu blueschist, NW China. Precambrian Research, 326, 295–311. doi: 10.1016/j.precamres.2017.12.041.

Xiao YY, Fan TL, Yu BS. 2011. Geochronological implication of the diabase intrusion into the Sinian strata in Northwest Tarim Basin. Special Oil and Gas Reservoirs, 18(5): 21 –25 (in Chinese with English abstract). doi: 10.1016/S1003-9953(10)60145-4

Xu B, Jian P, Zheng H, Zou H, Zhang L, Liu D. 2005. U-Pb zircon geochronology and geochemistry of Neoproterozoic volcanic rocks

in the Tarim block of Northwest China: Implications for the breakup of Rodinia supercontinent and Neoproterozoic glaciations. Precambrian Research, 136, 107–123. doi: 10.1016/j.precamres.2004.09.007.

Xu B, Xiao S, Zou H, Chen Y, Li Z, Song B, Liu D, Zhou C, Yuan X. 2009. SHRIMP zircon U-Pb age constraints on Neoproterozoic Quruqtagh diamictites in NW China. Precambrian Research, 168, 247–258. doi: 10.1016/j.precamres.2008.10.008.

Xu B, Zou HB, Chen Y, He JY, Wang Y. 2013. The Sugetbrak basalts from northwestern Tarim block of northwest China: Geochronology, geochemistry and implications for Rodinia breakup and ice age in the Late Neoproterozoic. Precambrian Research, 236, 214–226. doi: 10.1016/j.precamres.2013.07.009.

Zhang CL, Yang DS, Wang HY, Takahashi Y, Ye HM. 2011. Neoproterozoic maficultramafic layered intrusion in Quruqtagh of northeastern Tarim block, NW China: Two phases of mafic igneous activity with different mantle sources. Gondwana Research, 19, 177–190. doi: 10.1016/j.gr.2010.03.012.

Zhang CL, Li XH, Li ZX, Lu SN, Ye HM, Li HM. 2007. Neoproterozoic ultramafic-mafic-carbonatite complex and granitoids in Quruqtagh of northeastern Tarim block, western China: Geochronology, geochemistry and tectonic implications. Precambrian Research, 152, 149–169. doi: 10.1016/j.precamres.2006.11.003.

Zhang CL, Li ZX, Li XH, Wang AG, Guo KY. 2006. Neoproterozoic bimodal intrusive complex in southwestern Tarim block of NW China: Age, geochemistry and Nd isotope and implications for the rifting of Rodinia. International Geology Review, 48, 112–128. doi: 10.2747/0020-6814.48.2.112.

Zhang CL, Li ZX, Li XH, Ye HM. 2009. Neoproterozoic mafic dyke swarm in north margin of the Tarim, NW China: age, geochemistry, petrogenesis and tectonic implications. Journal of Asian Earth Sciences, 35, 167–179. doi: 10.1016/j.jseaes.2009.02.003.

Zhang CL, Shen JL, Guo KY. 2004. Geochemistry of the Neoproterozoic mafic dyke swarm and basalt in south of Tarim Plate and its tectonic significance. Acta Petrologica Sinica, 20, 473–482 (in Chinese with English abstract).

Zhang CL, Yang DS, Wang HY, Yutaka Takahashi Y, Ye HM. 2011. Neoproterozoic mafic-ultramafic layered intrusion in Quruqtagh of northeastern Tarim block, NW China: Two phases of mafic igneous activity with different mantle sources. Gondwana Research, 19, 177–190.

Zhang ZC, Kang JL, Kusky T, Santosh M, Huang H, Zhang DY, Zhu J. 2012. Geochronology, geochemistry and petrogenesis of Neoproterozoic basalts from Sugetbrak, northwest Tarim block, China: implications for the onset of Rodinia supercontinent breakup. Precambrian Research, 220–221, 158–176. doi: 10.1016/j.precamres.2012.08.002

Zhang CL, Zou HB, Li HK, Wang HY. 2013. Tectonic framework and evolution of the Tarim Block in NW China. Gondwana Research, 23, 1306–1315. doi: 10.1016/j.gr.2012.05.009.

Zhang ZY, Zhu WB, Shu LS, Su JB, Zheng BH. 2009. Neoproterozoic ages of the Kuluketage diabase dyke swarm in Tarim, NW China, and its relationship to the breakup of Rodinia. Geological Magazine, 146, 150–154. doi: 10.1017/S0016756808005839.

Zhu GY, Yan HH, Chen WY, Lei Y, Zhang, K J, Li TT, Chen ZY, Wu GH, Santosh M. 2020. Discovery of Cryogenian interglacial source rocks in the northern Tarim, NW China: Implications for Neoproterozoic paleoclimatic reconstructions and hydrocarbon exploration. Gondwana Research, 80, 370–384. doi: 10.1016/j.gr.2019.10.016.

Zhu WB, Zhang ZY, Shu LS, Lu HF, Su JB, Yang W. 2008. SHRIMP U-Pb zircon geochronology of Neoproterozoic Korla mafic dykes in the northern Tarim Block, NW China: Implications for the long-lasting breakup process of Rodinia. Journal of the Geological Society London, 165, 887–890. doi: 10.1144/0016-76492007-174.

Zhu WB, Zheng BH, Shu LS, Ma DS, Wu HL, Li YX, Huang WT, Yu JJ. 2011. Neoproterozoic tectonic evolution of the Precambrian Aksu blueschist terrane, northwestern Tarim, China: Insights from LA-ICP-MS zircon U-Pb ages and geochemical data. Precambrian Research, 185, 215–230. doi: 10.1016/j.precamres.2011.01.012.

Zindle A, Hart SR. 1986. Chemical geodynamics. Annual Review of Earth and Planetary Sciences, 14, 493–571. doi: 10.1146/annurev.ea.14.050186.002425.